SWISS COMPETENCE CENTER for ENERGY RESEARCH
SUPPLY of ELECTRICITY

Characteristics of seismic wavefields in fluid-saturated fractured rocks

University of Lausanne, Switzerland
Università della Svizzera Italiana, Switzerland

Institute of Petroleum Geology and Geophysics SB RAS , Novosibirsk, Russia
CONICET, Centro Atómico Bariloche – CNEA, Argentina

UNIL | Université de Lausanne

Università della Svizzera italiana
Institute of Computational Science ICS

Motivation

Characteristics of fractured media from seismic wavefields

Measurement:
Recorded seismic wavefield

→

Seismic Attributes:
Velocities
Attenuation
Anisotropic parameters

⇢

Properties of the fractured medium

Physical Mechanisms?

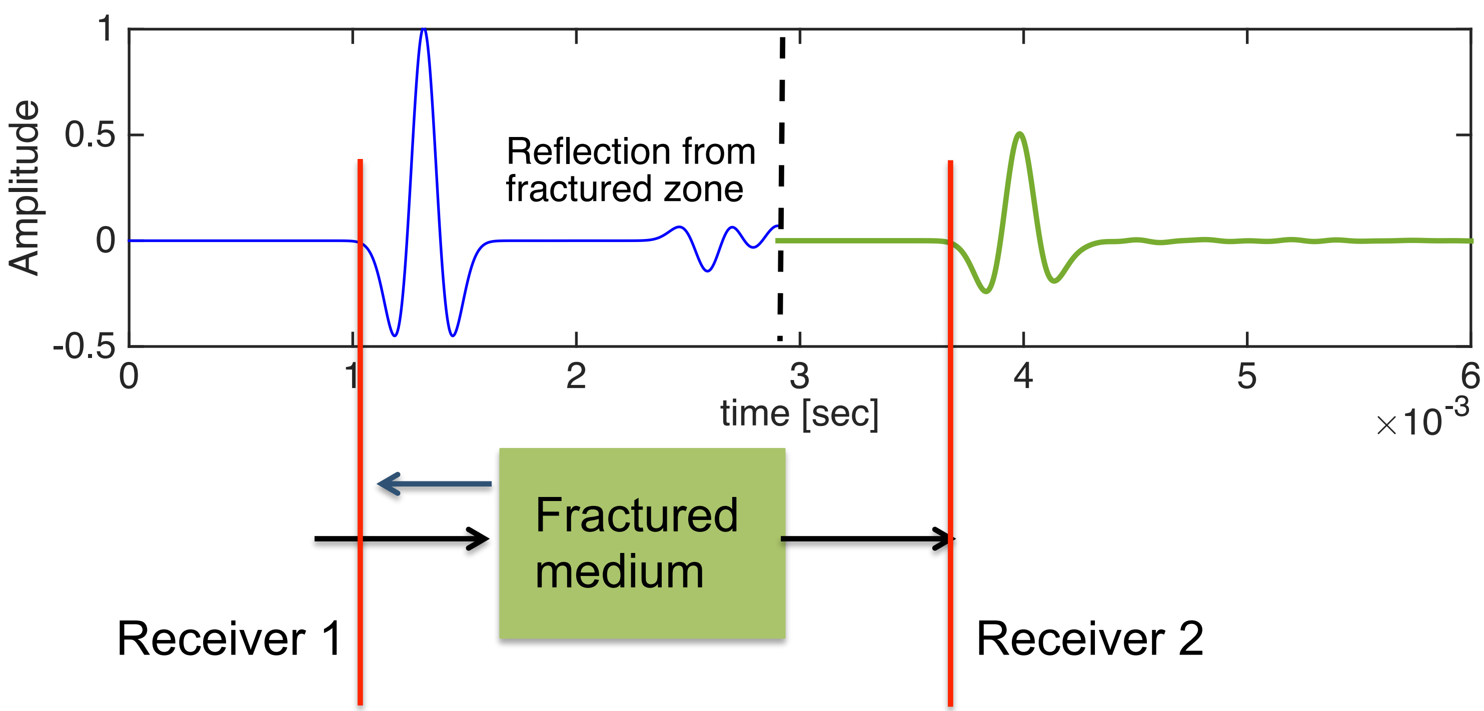

Scales

Laboratory data | Log data | Seismic data (VSP)

MHz — Measurement frequency – seismic wavelength — Hz

cm — Spatial scales (fracture dimension) — km

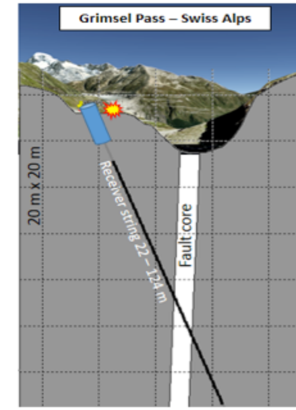

"Despite these striking scale differences the physical mechanisms are similar "

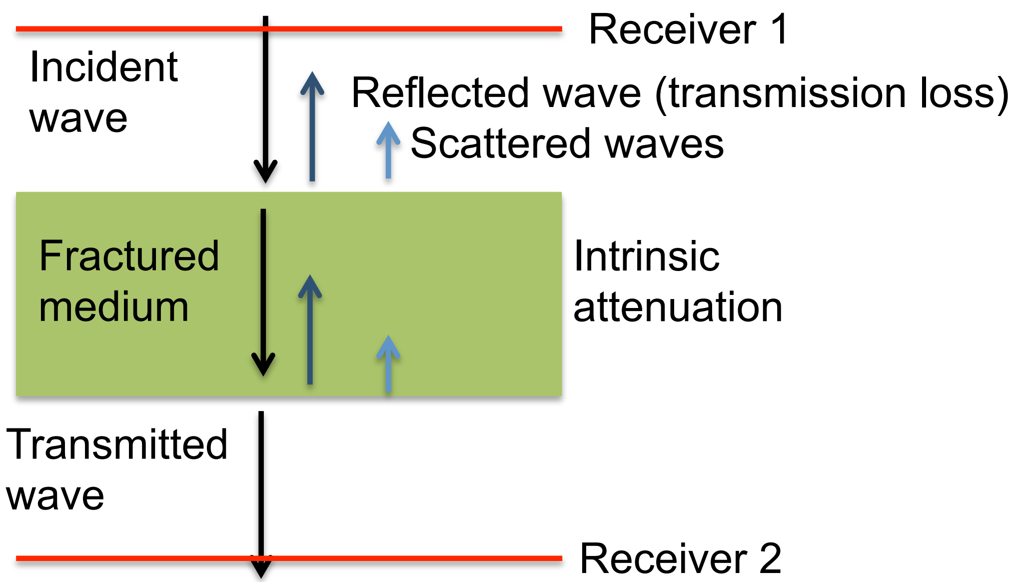

Attenuation

$$Q_p^{-1}(\omega) =$$

$$Q_{transmission}^{-1}(\omega)$$

$$+Q_{scattering}^{-1}(\omega)$$

$$+Q_{intrinsic}^{-1}(\omega)$$

Outline

Can we link intrinsic attenuation to fracture network properties?

Numerical upscaling approach applied to stochastic fracture networks

- ➢ Wave propagation effects are ignored

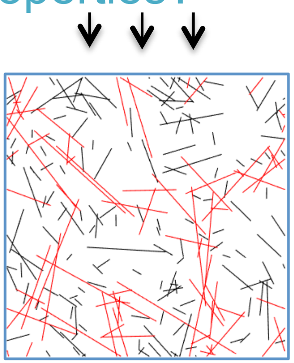

The role played by wave propagation effects

A comparison of wave propagation modelling and numerical upscaling for simple models

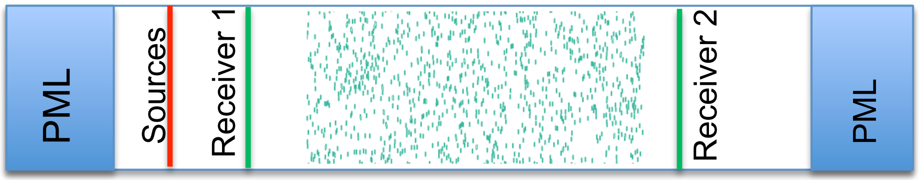

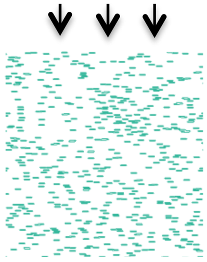

Application to full wave-form sonic data

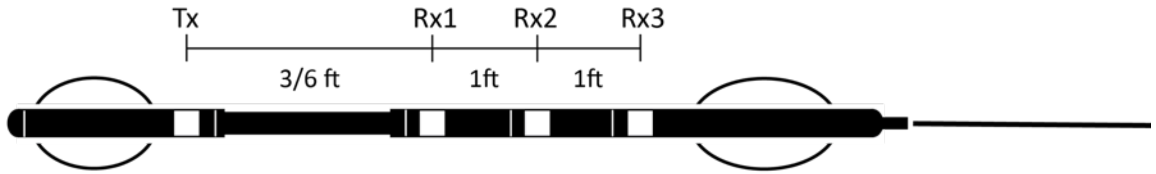

Intrinsic attenuation – in fractured fluid saturated media

Background: stiff porous matrix of low porosity and permeability

Fractures: compliant inclusion of high porosity and permeability

Mechanism: Pressure diffusion processes (fractures << seismic wavelength)

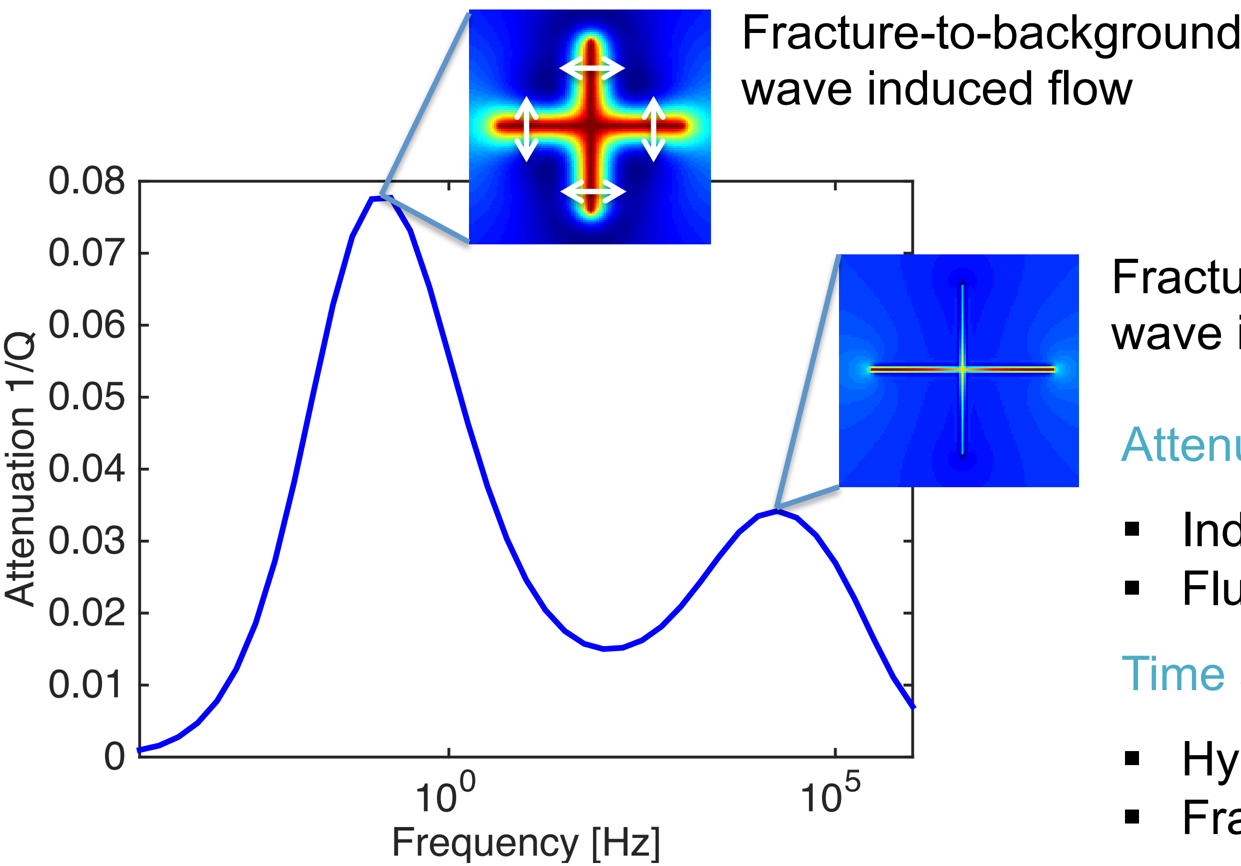

Attenuation magnitude:

- Induced pressure gradients
- Fluid storage volume

Time scale (frequency)

- Hydraulic properties
- Fracture size

Stochastic fracture networks

Fracture network parameter: $$n(l,L) = d_{frac}(a-1)\frac{l^{-a}}{l_{\min}^{-a+1}} \quad \text{for } l \in [l_{\min}, l_{\max}]$$

Constant aperture

Variable aperture

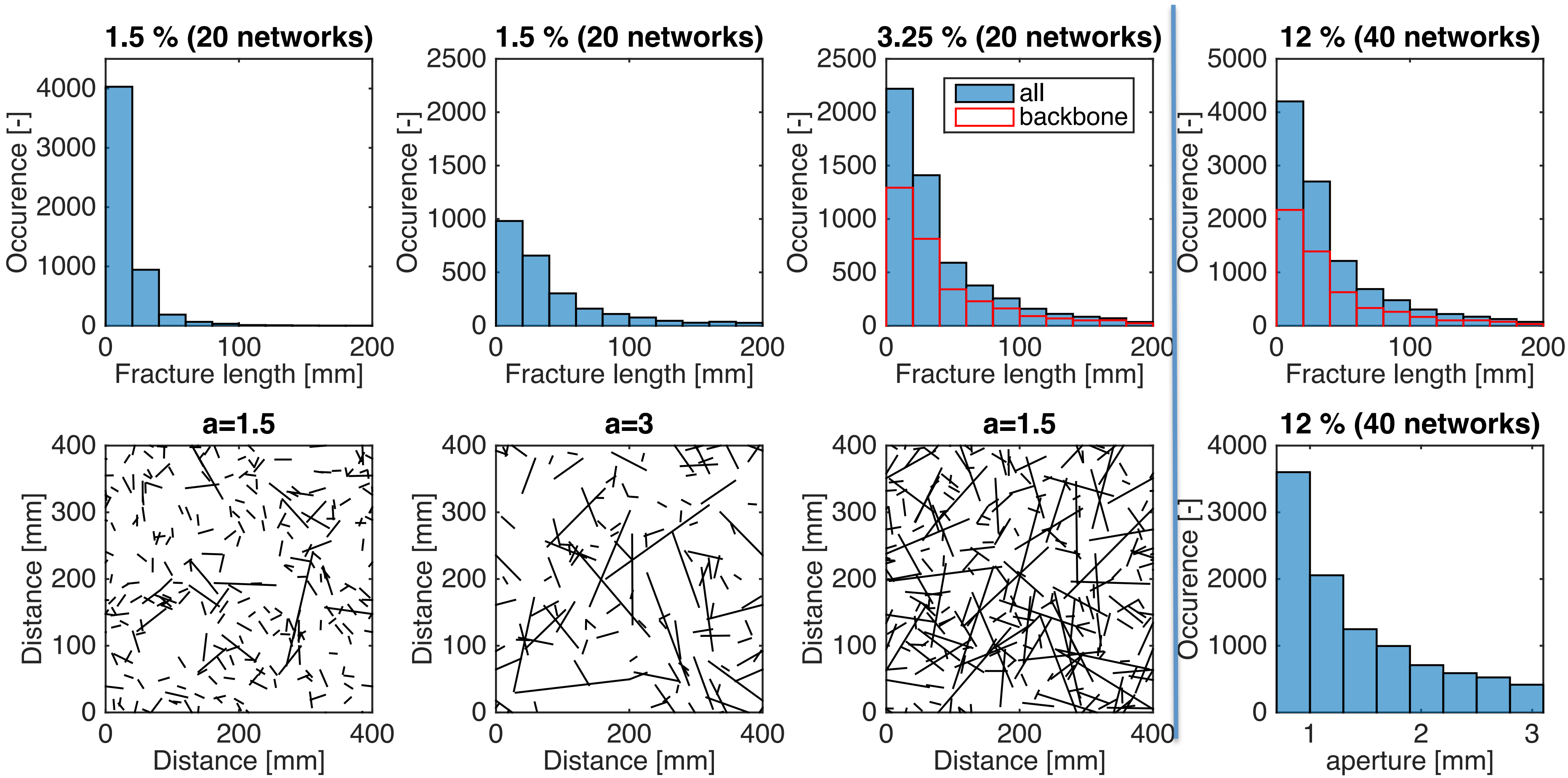

Pressure fields

a= 1.5

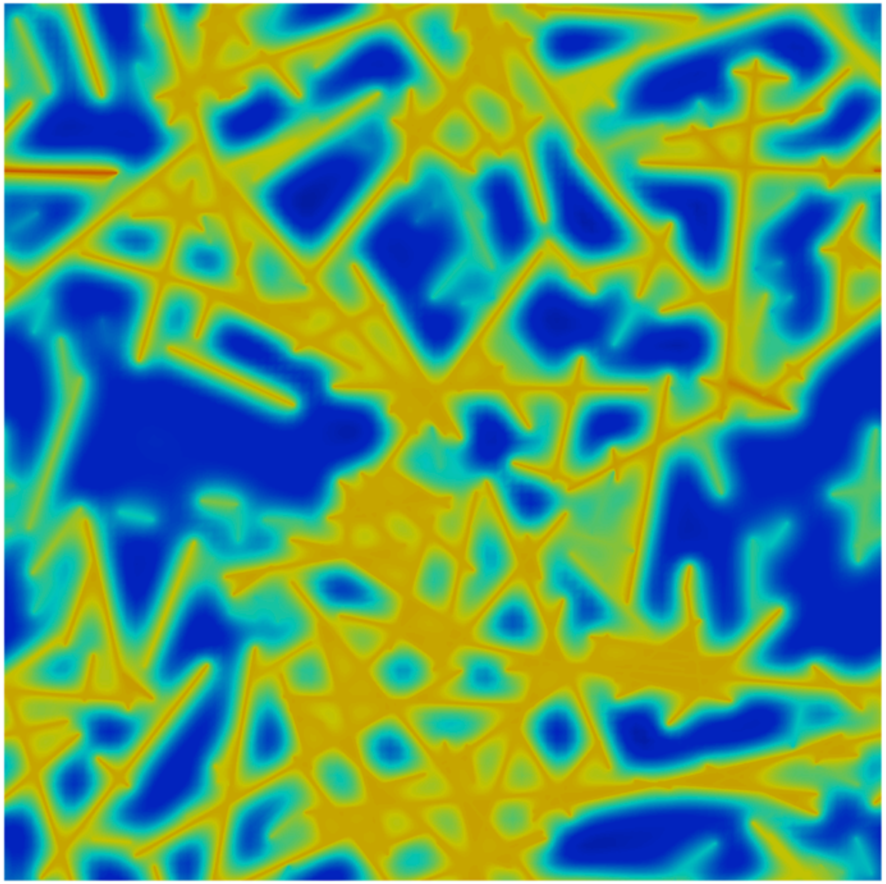

a=3

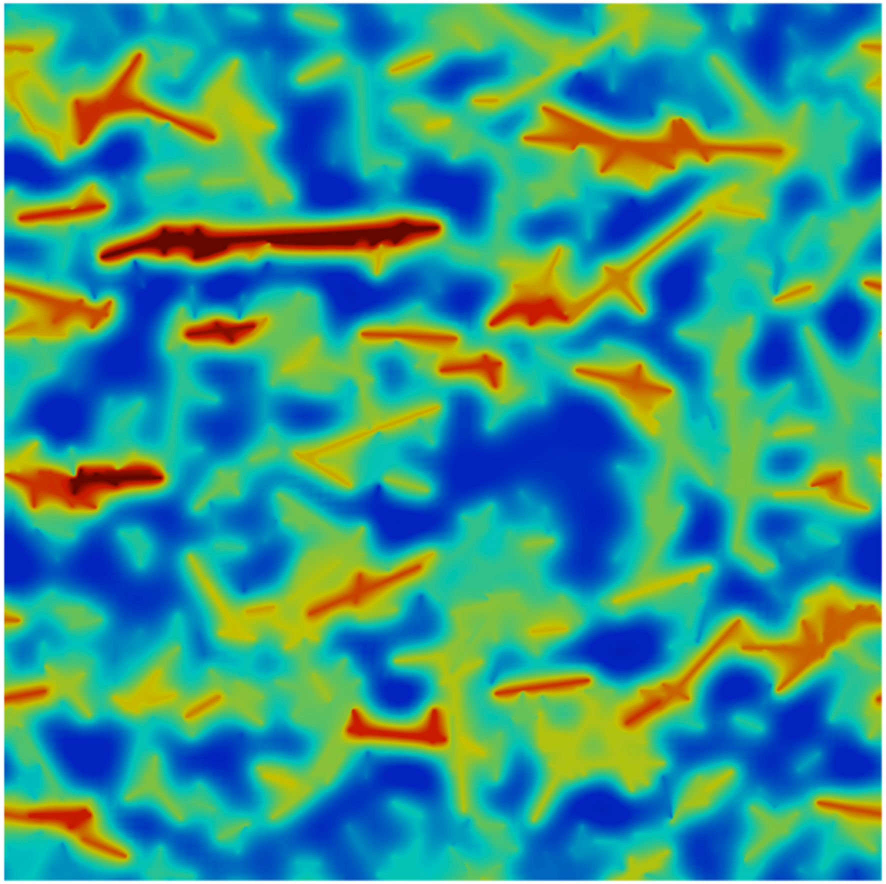

Attenuation trends: length distribution and fracture volume

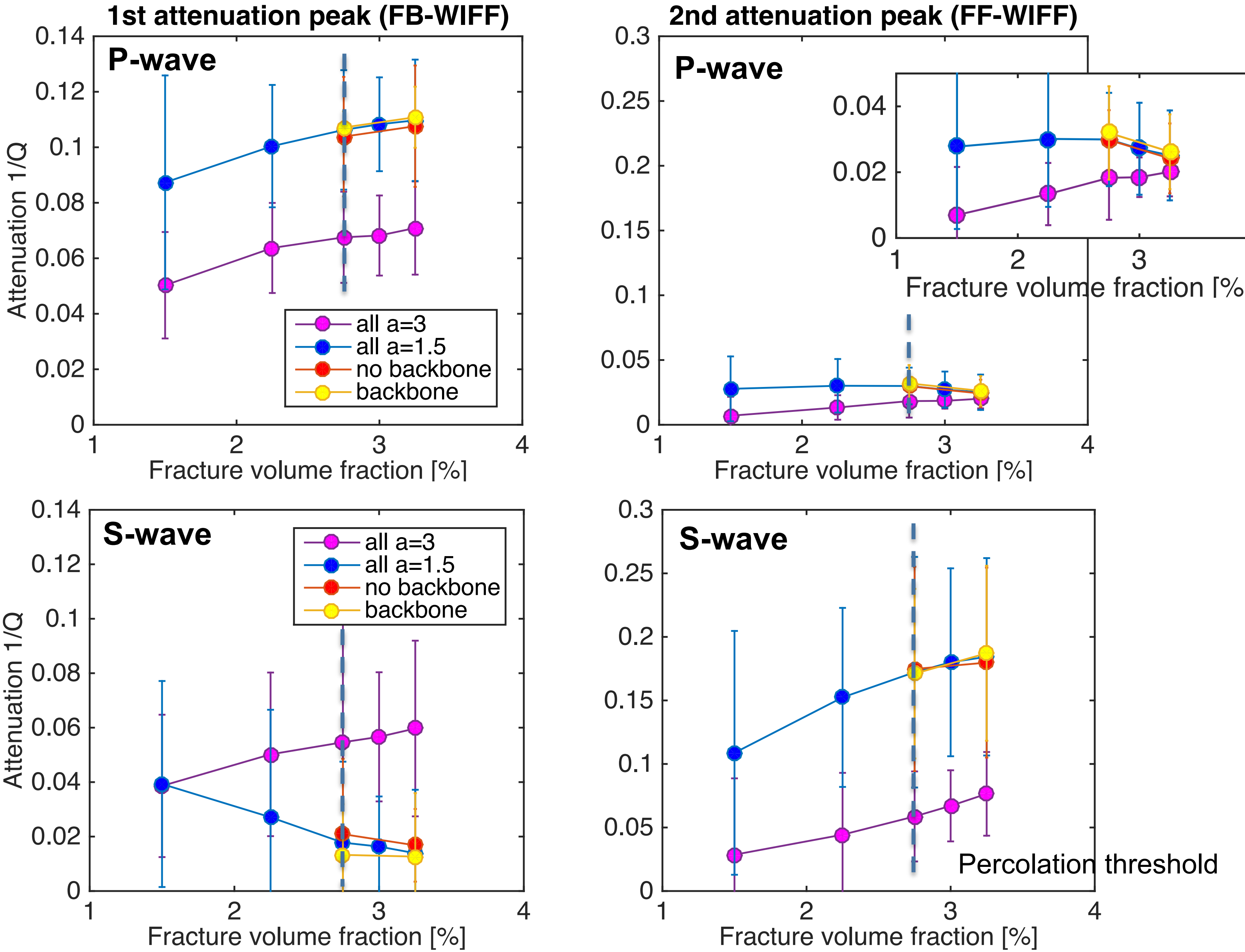

Comparison constant vs. variable aperture: Attenuation trends vs. fracture volume

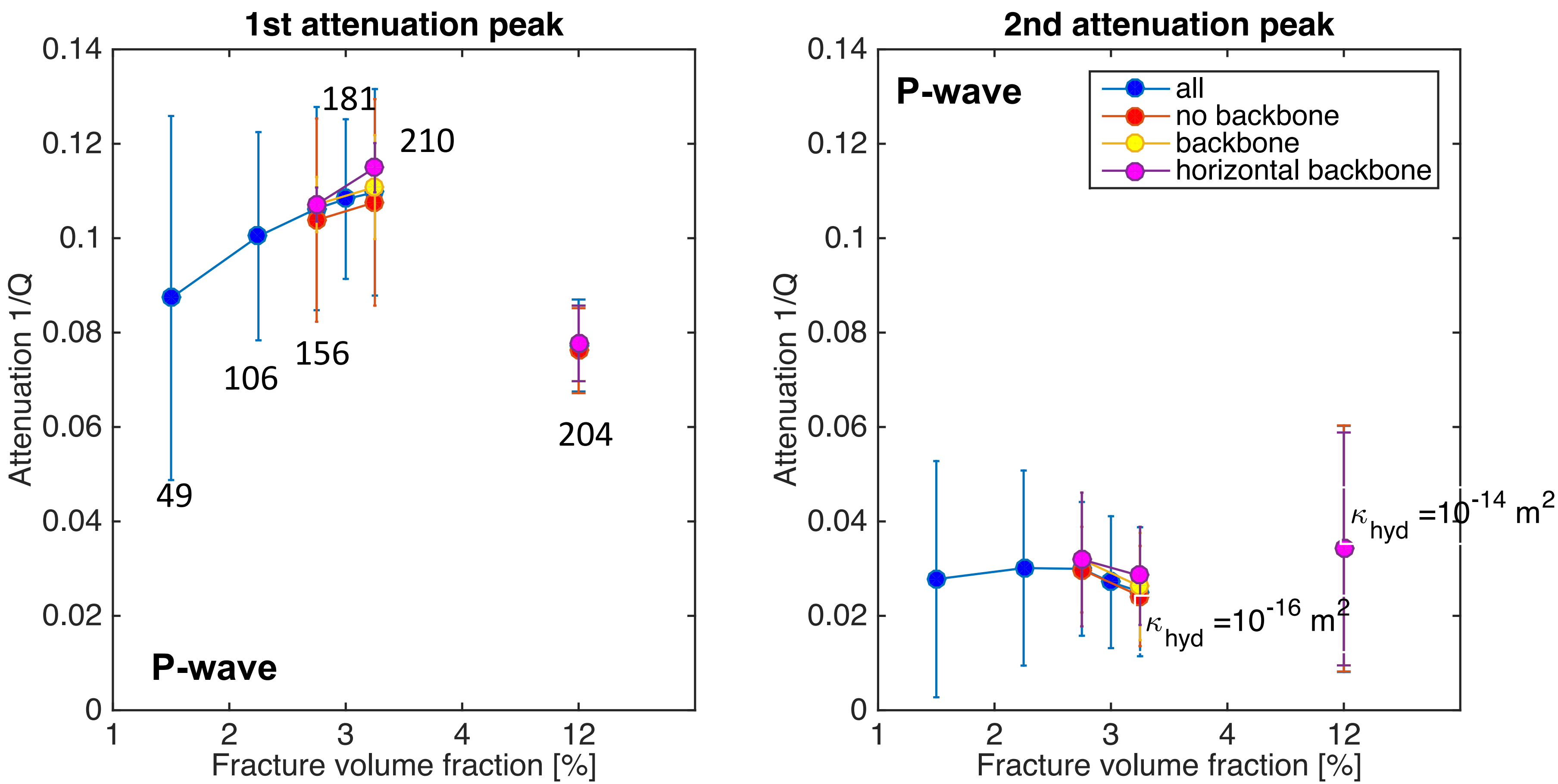

Fracture-to-fracture flow: Increase with fluid storage volume within fractures (larger apertures!) but not necessarily number of connections!

Conclusions

➔Establishing a direct relation between hydraulic conductivity and attenuation remains difficult !

Seismic attenuation depends on:

- Number of local connections
- Size of fracture cluster
- Fluid storage volume
- Elastic interaction between fractures
- Fracture length distribution
- Orientation of fractures (isotropic networks)

➔ P-wave attenuation trends change close to percolation threshold

➔ Sensitive to the degree of local fracture network connectivity but not to the existence of a backbone !

➔ Differing P- and S-wave attenuation trends are a possible indicator of fracture connectivity

Wave propagation effects: Oscillatory test vs transmission experiment

Numerical upscaing based on Biot's quasi-static equations (QS)

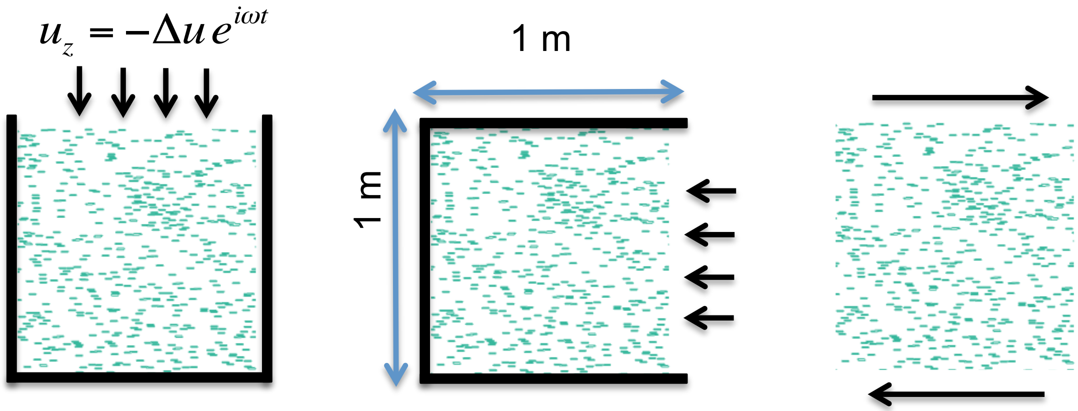

Pressure diffusion:
FB-WIFF
FF-WIFF

Wave propagation modelling based on Biot's dynamic equations (WP)

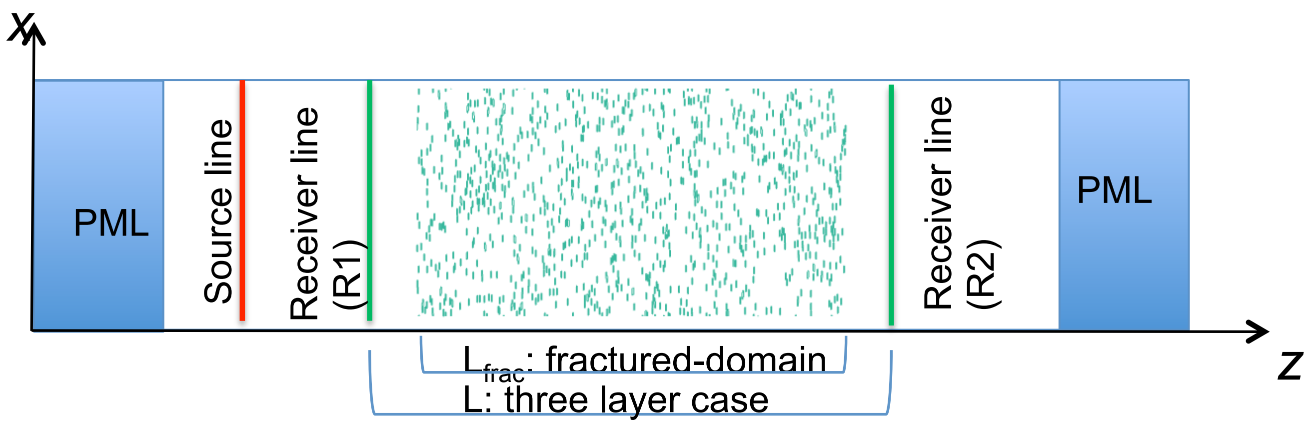

Pressure diffusion
Biot global flow

Scattering
Transmission losses

Domain size: 2 - 5 wavelengths (20 correlation lengths of the medium)

Attenuation and velocity estimation

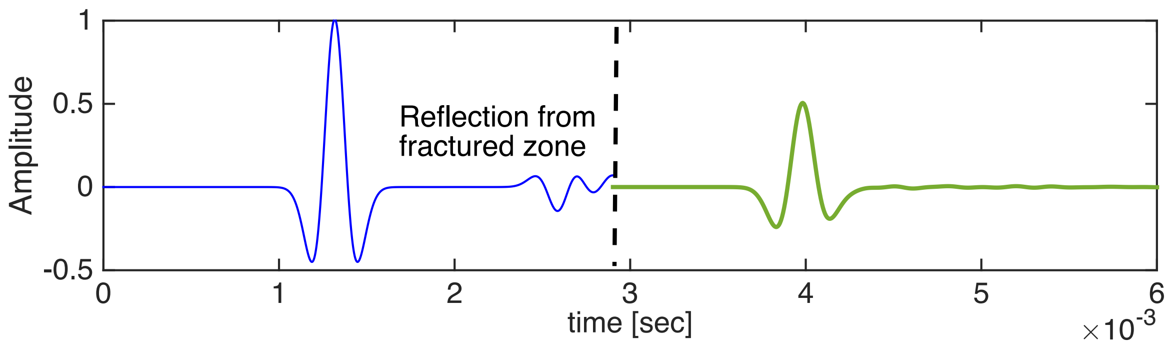

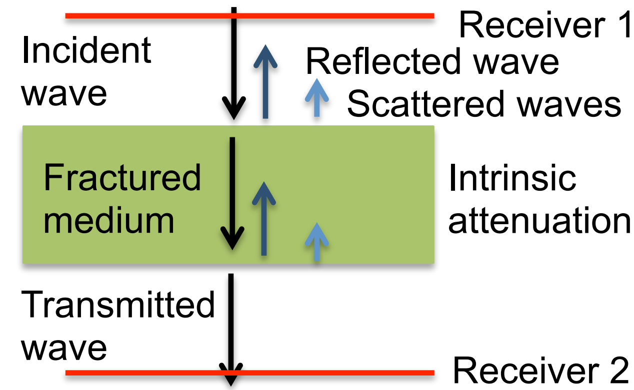

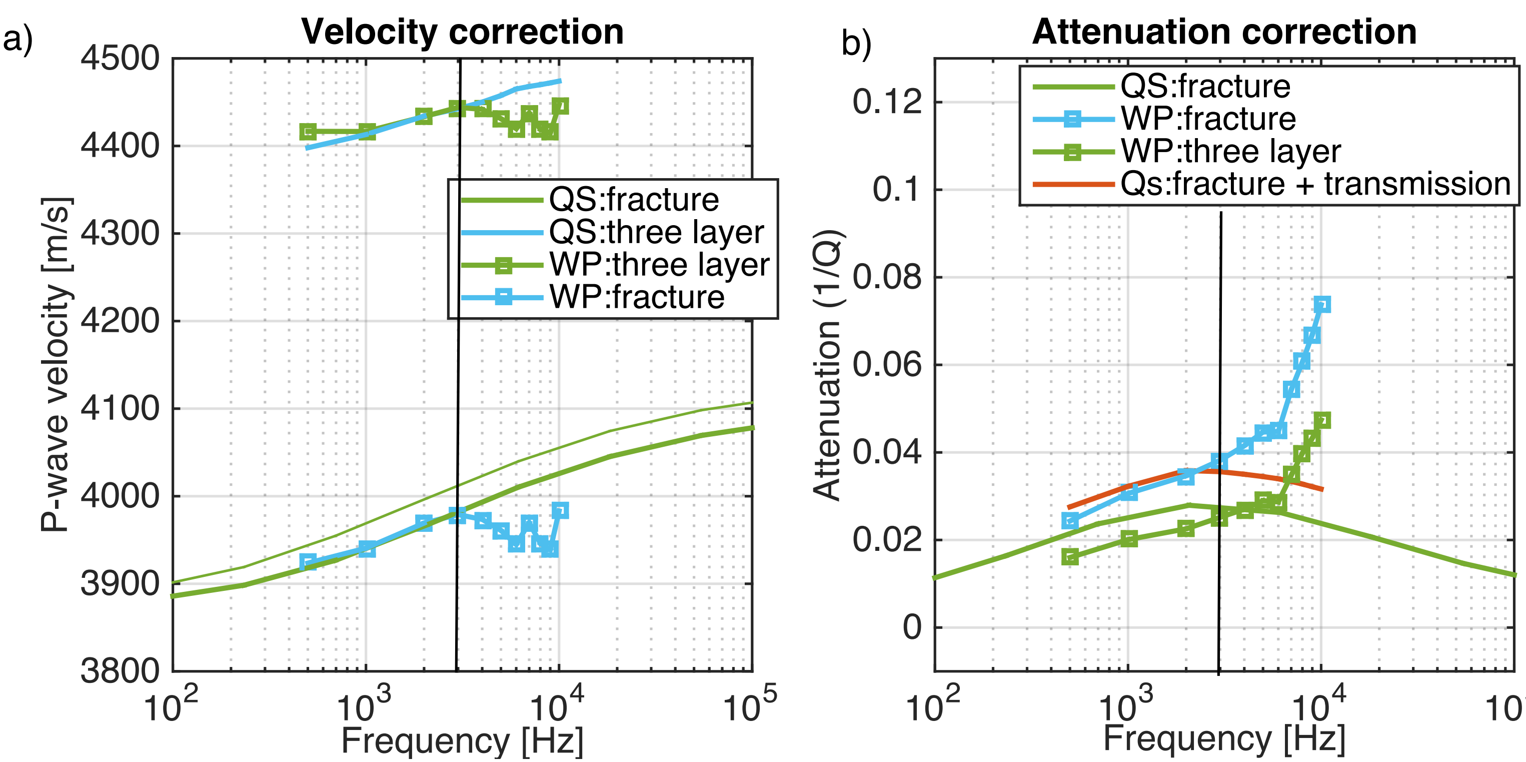

$$Q_p^{-1}(\omega) = Q_{transmission}^{-1}(\omega) + Q_{scattering}^{-1}(\omega) + Q_{intrinsic}^{-1}(\omega)$$

Full-waveform sonic log measurements – Grimsel Felslabor (INJ2)

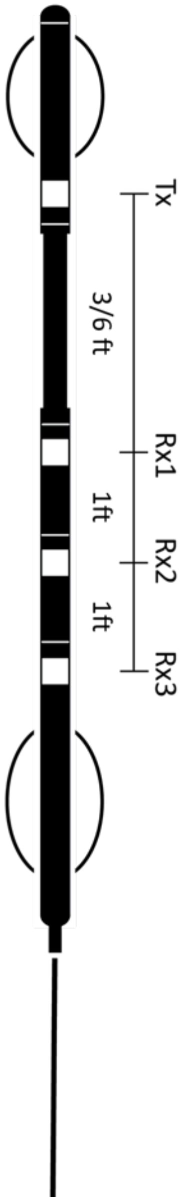

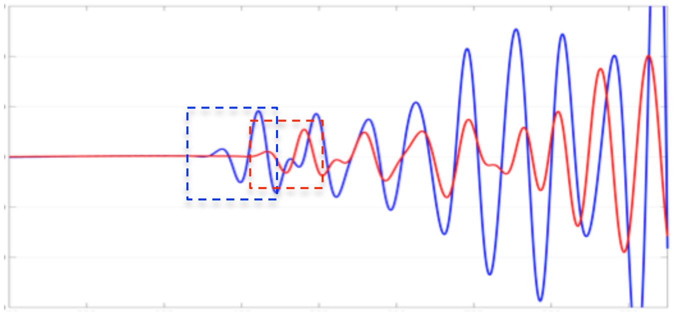

$$Q_p^{-1}(\omega) = Q_{spreading}^{-1}(\omega) + Q_{intrinsic}^{-1}(\omega) + \boxed{Q_{transmission}^{-1}(\omega)}$$

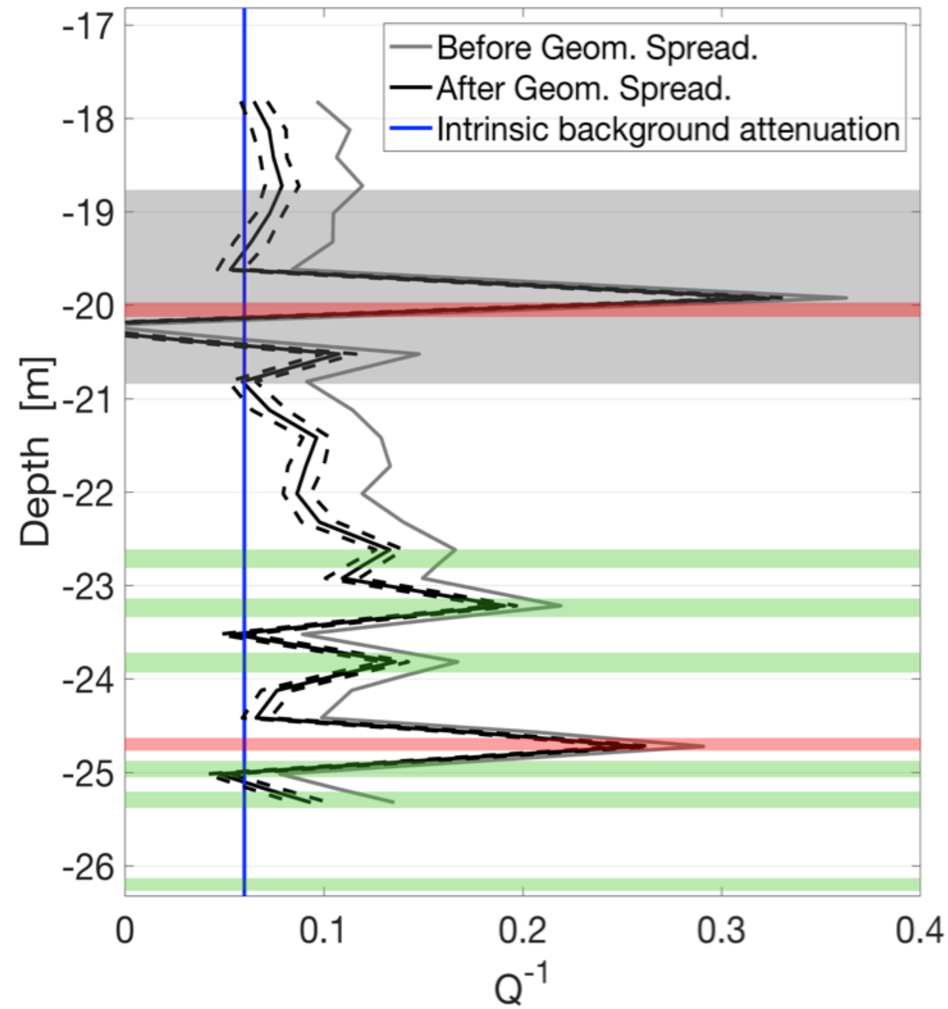

Transmission coefficients and fracture compliance

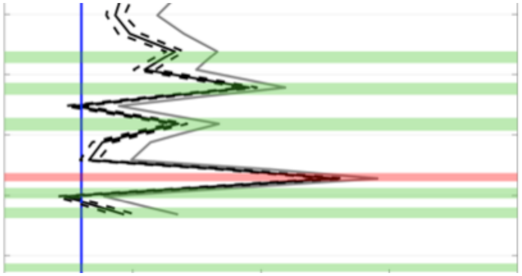

+ Velocities → Transmission coefficient → Fracture compliance

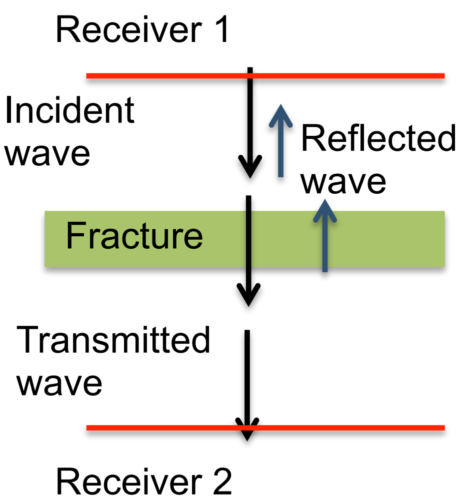

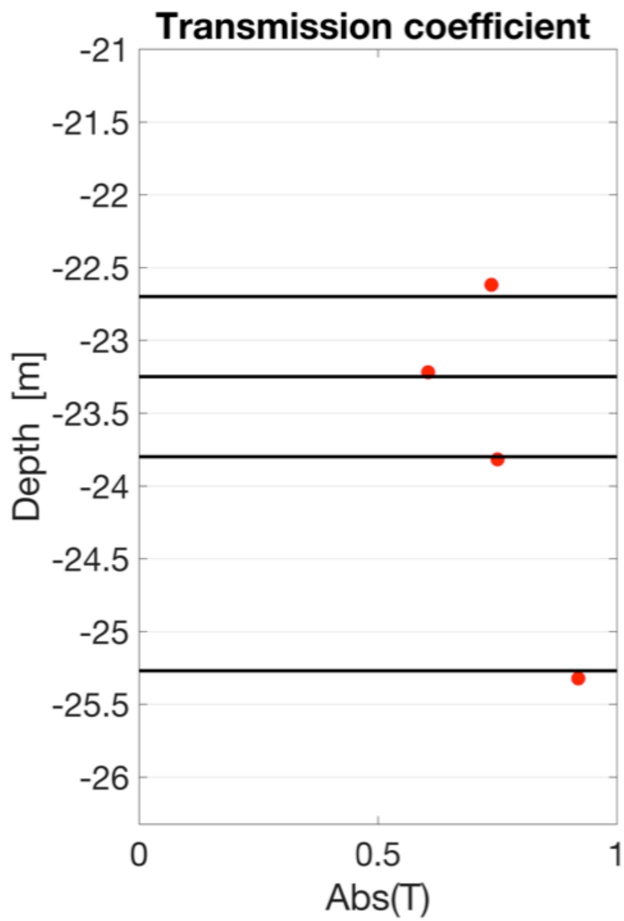

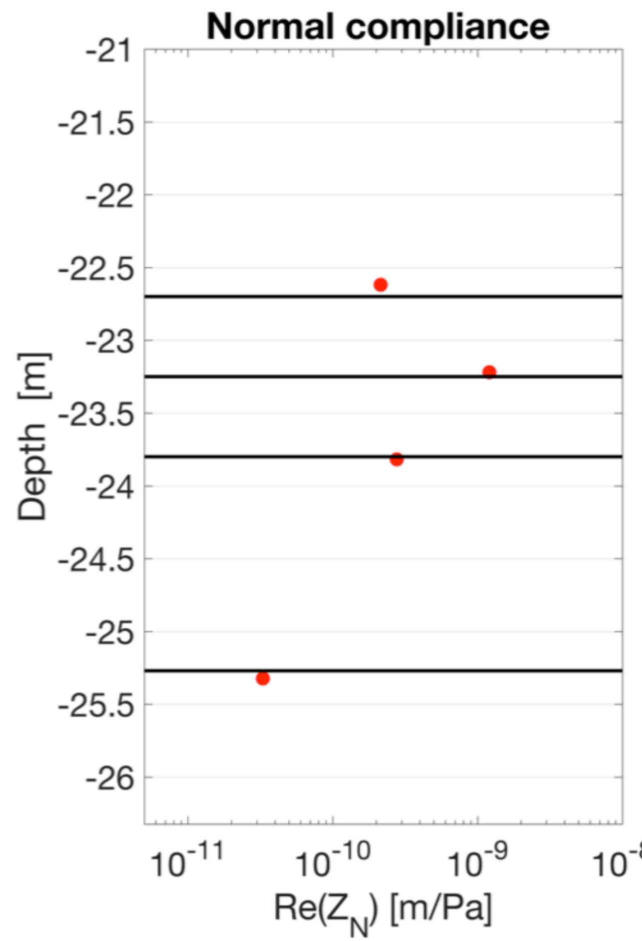

Poster

Seismic attenuation in porous rocks containing stochastic fracture networks: Jürg Hunziker, Marco Favino, Eva Caspari, Beatriz Quintal, J. Germán Rubino, Rolf Krause and Klaus Holliger

Attenuation in fluid-saturated fractured porous media – quasi-static numerical upscaling vs dynamic wave propagation modeling: Eva Caspari, Mikhail Novikov, Vadim Lisitsa, Nicolás D. Barbosa, Beatriz Quintal, J. Germán Rubino and Klaus Holliger

Seismic transmissivity of fractures from full-waveform sonic log measurements: Nicolás D. Barbosa, Eva Caspari, J. Germán Rubino, Tobias Zahner, Andrew Greenwood, Ludovic Baron, Klaus Holliger

Efficient Finite Element Simulation Methods for Fracture Networks: Marco Favino, Jürg Hunziker, Klaus Hollliger, Rolf Krause

---

Towards fracture characterization using tube waves: Jürg Hunziker, Shohei Minato, Eva Caspari, Andrew Greenwood and Klaus Holliger

Characterization and imaging of a fractured crystalline hydrothermal fault zone from hydrophone VSP data: A. Greenwood, E. Caspari, J. Hunziker, L. Baron, and K. Holliger.

Geophysical characterization of a hydrothermally active fault zone in crystalline rocks – GDP 1 borehole, Grimsel Pass: Eva Caspari, Ludovic Baron, Tobias Zahner, Andrew Greenwood, Enea Toschini, Daniel Egli and Klaus Holliger

A numerical approach for studying attenuation in interconnected fractures: Beatriz Quintal, Eva Caspari, Klaus Holliger and Holger Steeb

Acknowledgements

This work has been completed within the Swiss Competence Center on Energy Research – Supply of Electricity with the support of the Swiss Commission for Technology and Innovation.

We are thankful to the Russian Foundation for Basic Research grants no. 16-05-00800, 17-05-00250, 17-05-00579 for financial support of the research. Simulations of seismic wave propagation were performed on clusters of the Siberian Supercomputer Center.

Numerical upscaling

Biot's (1941) quasi-static poroelastic equations:

$$\nabla \cdot \boldsymbol{\sigma} = 0,$$

$$i\omega \frac{\eta}{k} \mathrm{w} = -\nabla p$$

$$\boldsymbol{\sigma} = \left[\left(H - 2G \right) \nabla \cdot \mathrm{u} + \alpha M \nabla \cdot \mathrm{w} \right] \mathbf{I} + G \left[\nabla \mathrm{u} + \left(\nabla \mathrm{u} \right)^T \right],$$

$$-p = \alpha M \nabla \cdot \mathrm{u} + M \nabla \cdot \mathrm{w}$$

Compression test:

$$u_z = -\Delta u \, e^{i\omega t}$$

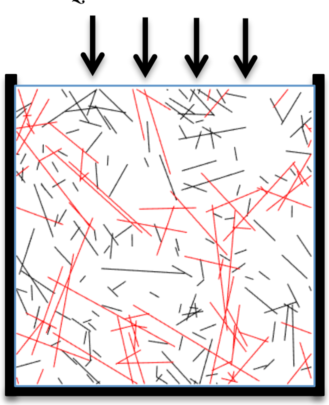

$$H(\omega) = \frac{\left\langle \sigma_{zz}(\omega) \right\rangle}{\left\langle \varepsilon_{zz}(\omega) \right\rangle}$$

$$Q_p^{-1}(\omega) = \frac{\Im(H(\omega))}{\Re(H(\omega))}$$

Simple shear test:

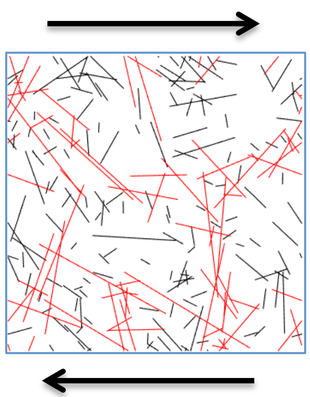

$$G(\omega) = \frac{\left\langle \sigma_{xz}(\omega) \right\rangle}{\left\langle 2\varepsilon_{xz}(\omega) \right\rangle}$$

$$Q_s^{-1}(\omega) = \frac{\Im(G(\omega))}{\Re(G(\omega))}$$

2D Wave propagation transmission experiment (time domain)

Biot's (1962) **dynamic** poroelastic equations (after Masson and Pride, 2010)

$$\nabla \cdot \boldsymbol{\sigma} = \rho \frac{\partial \mathbf{v}}{\partial t} + \rho_f \frac{\partial \mathbf{q}}{\partial t}$$

$$\rho_f \frac{T}{\phi} \frac{\partial \mathbf{q}}{\partial t} + \rho_f \frac{\partial \mathbf{v}}{\partial t} + \boxed{\frac{\eta}{k_0}} \mathbf{q} = -\nabla p$$

$$-\frac{\partial p}{\partial t} = M\left(\alpha \nabla \cdot \mathbf{v} + \nabla \cdot \mathbf{q}\right) + \mathbf{s}_f,$$

$$\frac{\partial \boldsymbol{\sigma}}{\partial t} = \left(\lambda_u \nabla \cdot \mathbf{v} + \alpha M \nabla \cdot \mathbf{q}\right)\mathbf{I} + \mu\left[\nabla \mathbf{v} + \left(\nabla \mathbf{v}\right)^T\right] + s.$$

Wave propagation transmission experiment:

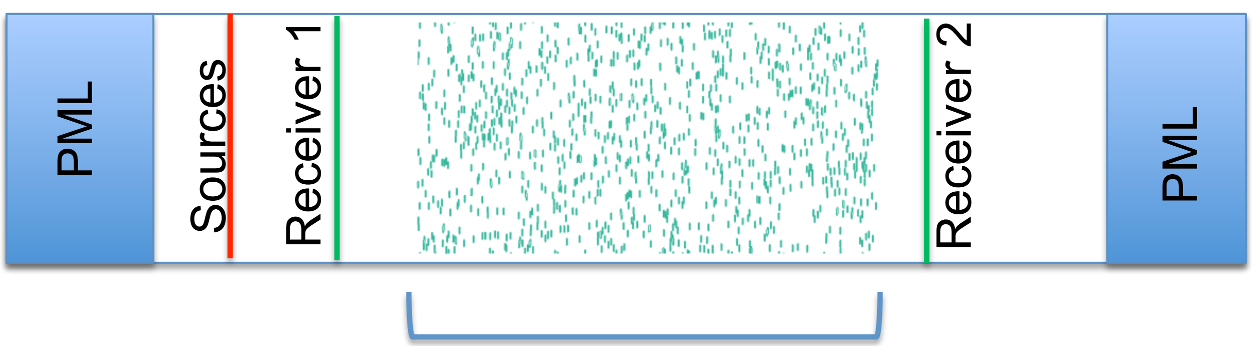

$\boxed{\frac{\eta}{k_0}}$ Steady limit of permeability: Neglects viscous boundary layers!

Domain size: 2 - 5 wavelengths (20 correlation lengths of the medium)

Attenuation: spectral-ratio type method

Fractured medium

Background: stiff porous matrix of low porosity and permeability

Fractures: compliant inclusion of high porosity and permeability

	Background	Fracture	Fluid
Bulk modulus [Gpa]	34	0.025	2.4
Shear modulus [GPa]	32	0.02	
Porosity	0.06	0.5	
Permeability [m^2]	10^{-18}	10^{-11} ($0.5\ 10^{-11}$ - 10^{-10})	

Fracture network parameter: Power law length distribution

$$n(l,L) = d_{frac}(a-1)\frac{l^{-a}}{l_{\min}^{-a+1}} \text{ for } l \ni [l_{\min}, l_{\max}]$$

	Constant	Variable
Exponent a	1.5	1.5
Length $l_{min,}$ l_{max} [mm]	10, 200	10, 200
Fracture volume d_{frac} [%]	1.5 – 3.25	12
Aperture [mm]	0.5	0.7 - 3

Constant aperture: P- and S-wave attenuation

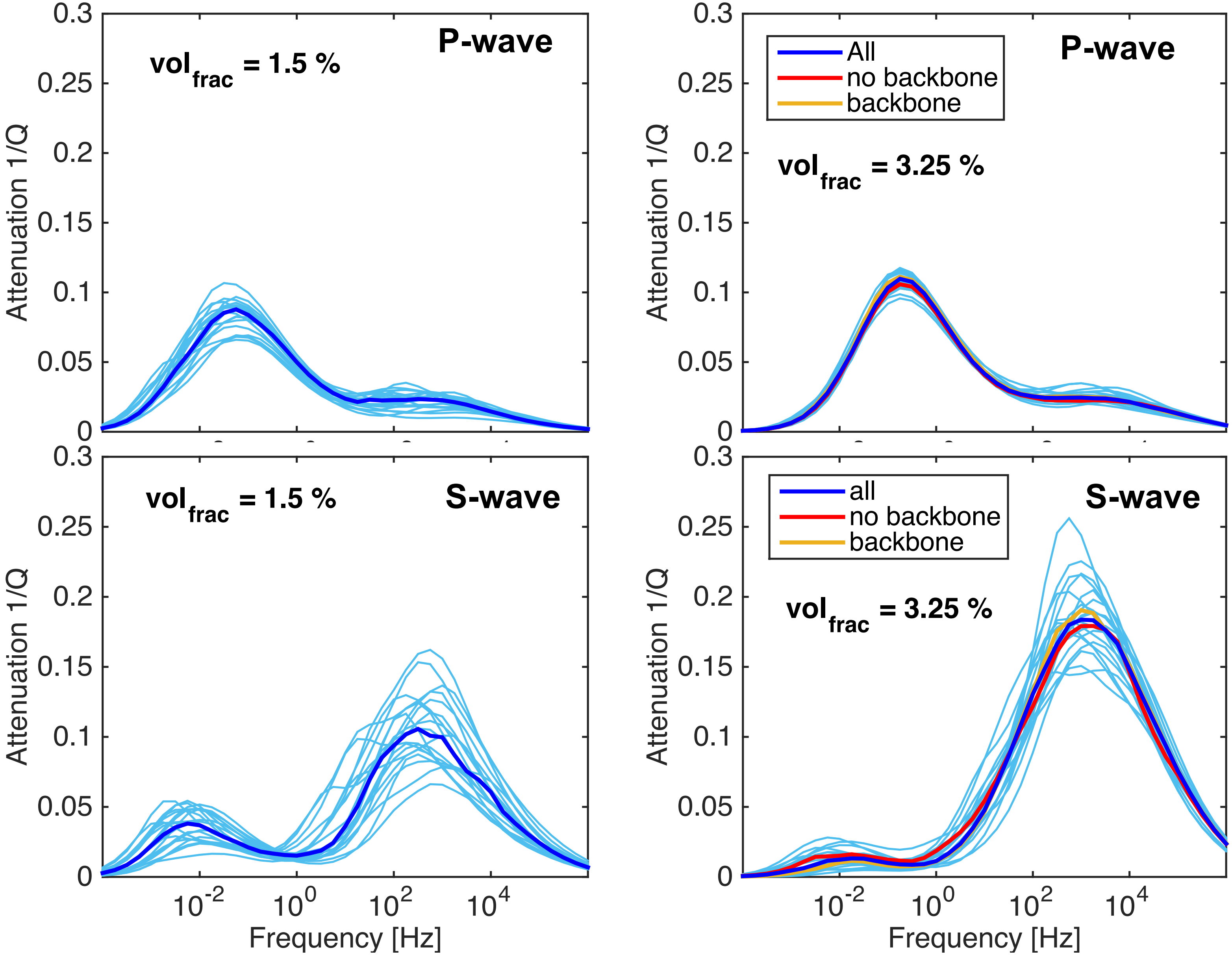

Fracture-to-background flow is dominant for P-waves

Fracture-to-fracture flow is dominant for S-waves

Pressure fields

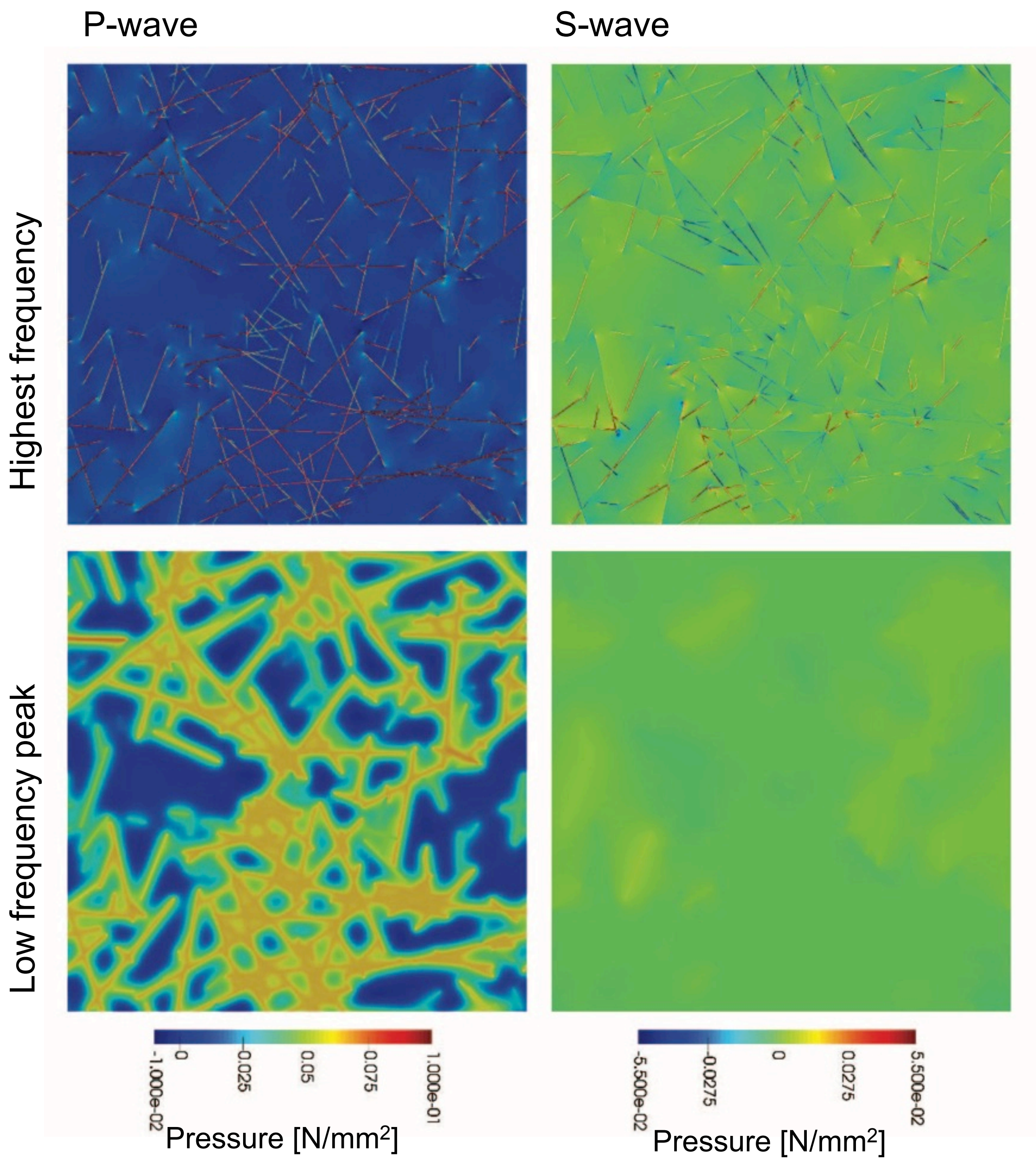

Fracture-to-fracture flow is dominant for S-waves

➔Larger induced pressure gradients

Fracture-to-background flow is dominant for P-waves

➔Larger remaining pressure gradients

Comparison constant vs. variable aperture: P-wave attenuation

Constant aperture

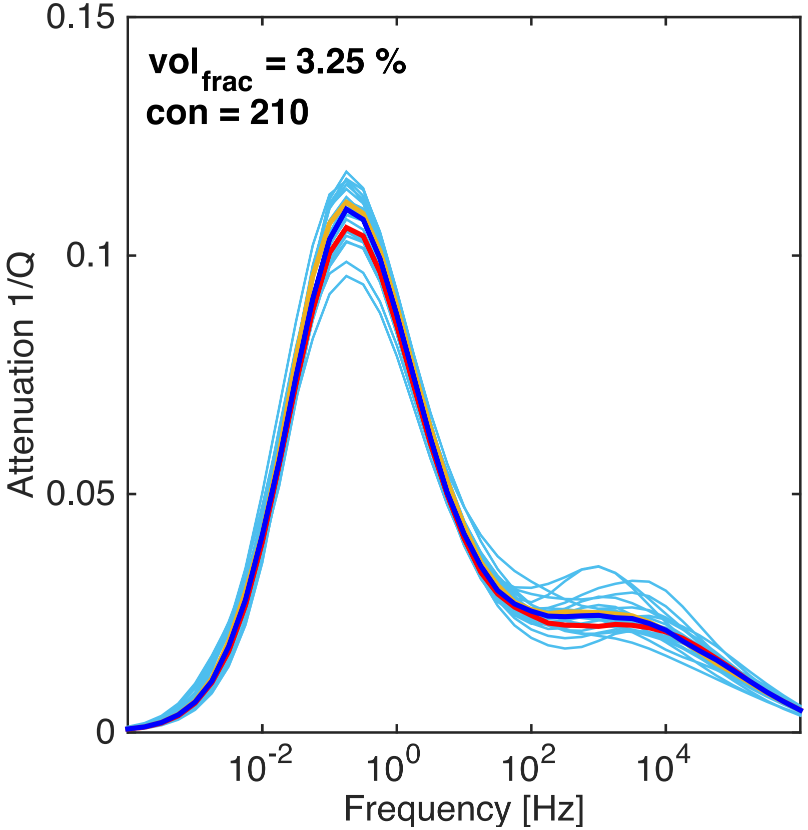

Variable aperture

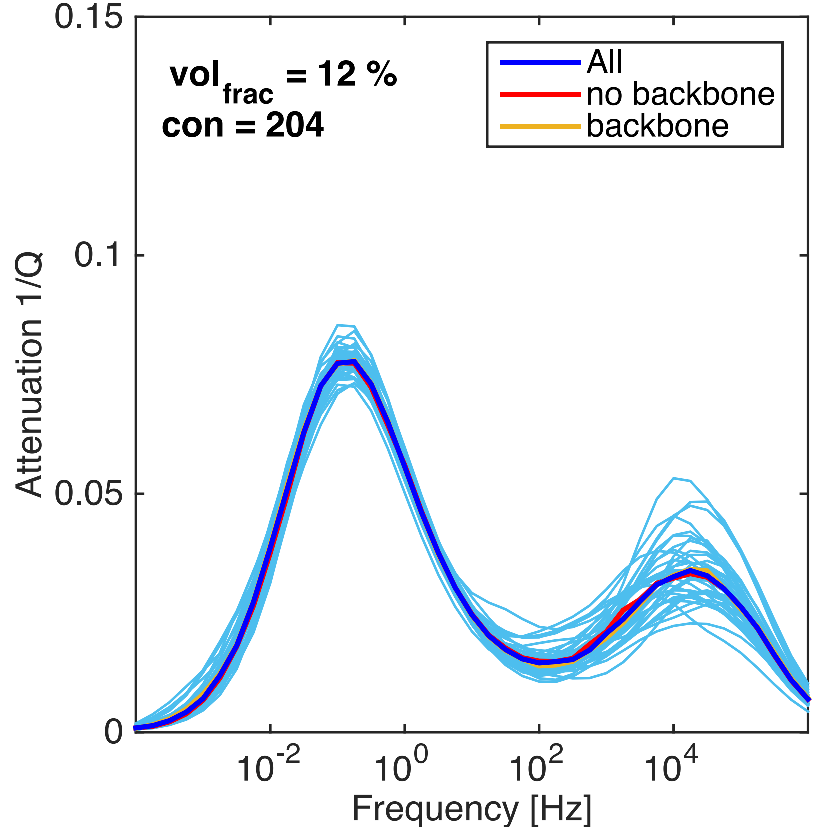

➔ Same degree of connectivity

➔ Increase in fluid storage volume within fractures (larger apertures!)